*Materials Transactions*, Vol. 56, No. 11 (2015) pp. 1905 to 1910

**EXPRESS REGULAR ARTICLE**

# The Thermal Stability and Strength of Highly Alloyed $Ni_3Al$

Te-Kang Tsao and An-Chou Yeh*

*Department of Materials Science and Engineering, National Tsing Hua University, Hsinchu, 30013, Taiwan R.O.C.*

In this study the $L1_2$ gamma prime phase (based on $Ni_3Al$) has been highly alloyed with Cr, Co, W, and Ta in order to examine the effects on strengthening and thermal stability. The order-disorder transition temperature of gamma prime is decreased with higher alloying content. Thermodynamic calculations show that the ordering enthalpy decreases as the entropy term increases. Conversely, the hardness can be 1.5 times higher comparing to that of a conventional Ni-based superalloy. This indicates that the strengthening effect of designing a gamma prime composition toward higher entropy is significant, due to greater lattice distortion and higher anti-phase boundary energy of gamma prime.
[doi:10.2320/matertrans.M2015298]

(Received July 24, 2015; Accepted September 3, 2015; Published October 25, 2015)

***Keywords:*** *superalloy, gamma prime, thermal stability, hardness*

## 1. Introduction

Superalloys are widely used in high temperature environments, having the ability to tolerate the harsh working environments with high temperature and pressure. They exhibit a unique combination of good high-temperature strength, oxidation resistance, corrosion resistance and toughness.[1–5] Among various kinds of superalloys, Nickel-based superalloy is the best choice of material for aero-engine and power generation applications due to their excellent phase stability and mechanical properties at high temperature. The typical microstructure of Ni-based superalloys is mainly composed of a FCC $\gamma$ matrix and a dispersion of ordered $L1_2$ $\gamma'$ precipitates. These $L1_2$ ordered structure precipitates play an important role in precipitation strengthening at high temperature. In order to further improve the high temperature mechanical properties of Ni-based superalloys, growing content of refractory elements like Mo and W have been added for solid-solution strengthening and to slow down the phase transformation rate, but this also results in the higher tendency for TCP phases formation. These TCP phases are brittle and have been reported to be detrimental to the thermal mechanical properties.[6,7] Re and Ru addition can enhance the creep resistance significantly,[8–11] however, the densities and costs of these additions are extremely high. Therefore, new approach for alloy strengthening with better cost-performance is still in demand.

A new alloy design concept called "high entropy alloy (HEA) approach" has been proposed.[12,13] HEA can achieve higher hardness and wear resistance, good oxidation and corrosion resistance[14–17] by severe lattice distortion and sluggish diffusion mechanisms.[18] These findings inspire us to study the composition of Ni-based superalloy toward higher entropy for the purpose of utilizing these special benefits in high entropy system. Since $\gamma'$ phase is vital for high temperature strengthening in Ni-based superalloys, it is intriguing to evaluate the influence of elevated mixing entropy ($\Delta S_{mix}$) on this important phase. Main elements in conventional Ni-based superalloy CM247LC, e.g. Co, Cr, Ta and W are chosen for alloying with $Ni_3Al$ in present work. From previous studies on the site preference of ternary additions in $Ni_3Al$,[19,20] it has been known that Ta and W substitute for Al site; Co and Cr prefer substituting for Ni site. Nevertheless, these studies only focus on small amount of alloying in $Ni_3Al$. Therefore, present study aims to enhance the mixing entropy of $Ni_3Al$ by multi-elemental additions with larger amount, not all the way into the high entropy alloy catagory. A systematic addition for the purpose of elevating $\Delta S_{mix}$ in $\gamma'$ phase have been conducted, and the phase stability, ordering property and strengthening mechanism will be discussed.

*Corresponding author, E-mail: yehac@mx.nthu.edu.tw

## 2. Experimental Procedure

### 2.1 Process and materials

$Ni_3Al$ and other two alloys with higher amount of equimolar Co, Cr, Ta and W addition were prepared by vacuum-arc-melting; they are designated as alloy A, B, and C. Pure Ni, Al, Co, Cr, Ta, W raw metal ingredients (purity better than 99 mass%) were melted in high-purity argon atmosphere and then solidified in a water-cooled copper mold. All samples were reversed and re-melted more than 4 times to assure chemical homogeneity. Specimens were cut from the button shape solidified ingots. The nominal composition of alloy A, B and C is $Ni_3Al$ with 0 at%, 4 at% and 8 at% Co, Cr, Ta, W addition, respectively and listed in Table 1. The metallographic specimens were prepared by typical grinding and polishing in sequence. The microstructure and composition examinations were carried out by scanning electron microscope (SEM, JEOL-5410) equipped with energy dispersive spectrometry (EDS, Oxford Instruments, Oxford, England) operating at 15 kV. The crystal structures were identified by X-ray diffractometer (Shimadzu

Table 1 Nominal and actual composition (at%) of alloy A, B, and C.

| alloy | | Ni | Al | Co | Cr | Ta | W |
|---|---|---|---|---|---|---|---|
| A | designed | 75.0 | 25.0 | — | — | — | — |
| | actual | 74.6 | 25.4 | — | — | — | — |
| B | designed | 63.0 | 21.0 | 4.0 | 4.0 | 4.0 | 4.0 |
| | actual | 62.4 | 20.8 | 4.0 | 4.4 | 3.7 | 4.7 |
| C | designed | 51.0 | 17.0 | 8.0 | 8.0 | 8.0 | 8.0 |
| | actual | 51.6 | 16.4 | 8.2 | 8.0 | 8.0 | 7.8 |

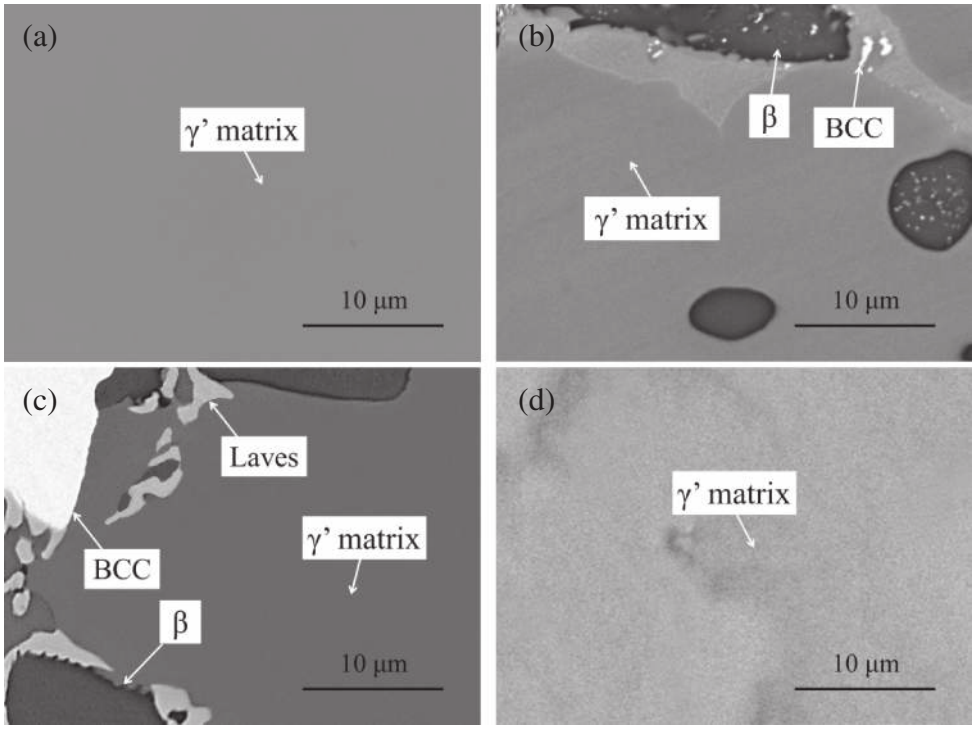


Fig. 1 The SEM images of as-cast alloy (a) A, (b) B, (c) C and (d) D.

XRD 6000) with Cu-target radiation at 30 kV and 20 mA. The XRD specimens were in plate form with dimension of 1 cm × 1 cm × 3 mm and scanned at $2\theta$ angle from 20 to 100° with a scanning rate of 2 deg/min. Pyris Diamond TG/DTA of the Perkin-Elmer Instruments was used to examine the thermal properties for all samples of 20–50 mg in an $Al_2O_3$ crucible, and tested from 1240 to 1400°C at a heating rate of 10°C/min under 400 sccm of Ar flow. Micro-hardness measurements were tested at room temperature by Mitutoyo HM-115 micro-hardness tester with loads of 25 g. The indentation was conducted on the $\gamma'$ phase region and the size of the indented area was 5–10 μm. The duration time in each indentation is 15 s, and five measurements on each sample were conducted to obtain an average value.

## 3. Results and Discussions

### 3.1 Microstructure and composition analysis

Table 1 lists the designed and actual composition measured by SEM-EDS of alloy A, B and C. Alloy A is the composition of $Ni_3Al$, and alloy B, C with 4 and 8 at% of Co, Cr, Ta, W addition. The actual composition is close to that of the designed ones, and the SEM images of as-cast alloy A, B and C are shown in Fig. 1.

According to these backscattered electron images, only single $\gamma'$ phase presents in alloy A, and in alloy B, $\beta$ phase appears as the black regions within the $\gamma'$ matrix along with other white regions as the W-rich BCC phase. As for alloy C, due to alloying beyond the solubility, the microstructure constituents are more complex with $\beta$, BCC phase and Laves phase, however, the matrix is still the $\gamma'$ phase. Figure 2 shows the XRD patterns of alloy A to C. Only ordered FCC peaks present in alloy A. Besides ordered FCC, $\beta$ and BCC phase peaks are present in alloy B. Alloy C contains all the characteristic peaks of alloy B with additional peaks of Laves phase. Consequently, the XRD results confirm that the ordered FCC $\gamma'$ phase present in these three alloys as the matrix phase.

The lattice constant of $\gamma'$ phase can be calculated from XRD results, and it shows an increasing trend from alloy A, B to C (0.3571, 0.3585 and 0.3592 nm, respectively). The lattice parameter of $Ni_3Al$ has been reported to be 0.357 nm,[21–25] which is close to that in present study. Mishima *et al.*[20] have studied the lattice parameter changes in $Ni_3Al$ with transition and B-subgroup elements addition; based on a linear relation between lattice constant and concentration of constituent at constant temperature, Vegard's Law was proposed for the prediction of $\gamma'$ lattice parameter in Ni-based superalloys. The value of $a_{\gamma'}$ is taken as 0.357 nm and the Vegard's coefficients of alloying elements for $\gamma'$ phase was obtained as the following formulae:

$$a_{\gamma'} = 0.357 - 0.0004X'_{Co} - 0.0004X'_{Cr} + 0.0208X'_{Mo} + 0.0194X'_{W} + 0.0258X'_{Ti} + 0.05X'_{Ta} + 0.046X'_{Nb}$$

According to Vegard's Law, Ta addition enhances the lattice parameter of $\gamma'$ significantly and so does W addition, while Co and Cr just slightly decrease it. Hence the increase in $\gamma'$ lattice constant from alloy A to C is reasonable due to the increasing alloying content of Ta and W. According to Vegard's Law, the $\gamma'$ lattice constants are 0.3597 and 0.3624 nm for alloy B and C, which are actually slightly higher than the XRD analyzed values (0.3585 and 0.3592 nm). It is possible that the presence of $\beta$, BCC, and Laves phase may constrain the ordered phase in present study.

The compositions of $\gamma'$ in alloy A, B and C are tabulated in Table 2, and the values of calculated mixing entropy ($\Delta S_{mix}$) are summarized in Fig. 3. The $\Delta S_{mix}$ is calculated from the following equation:

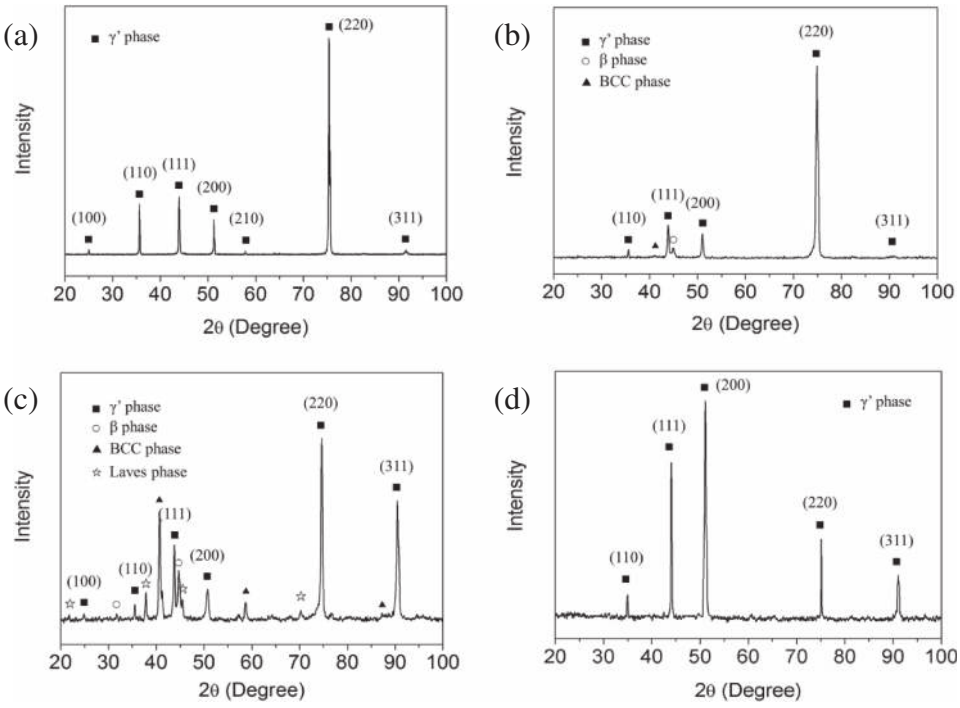


Fig. 2 The XRD results of as-cast alloy (a) A, (b) B, (c) C and (d) D.

Table 2 The $\gamma'$ composition (at%) of alloy A, B, C and some conventional Ni-based superalloys.

| $\gamma'$ composition | Ni | Al | Co | Cr | Ta | W | Ti | Mo | Re | Ru |
|---|---|---|---|---|---|---|---|---|---|---|
| alloy A | 74.6 | 25.4 | — | — | — | — | — | — | — | — |
| alloy B | 65.6 | 19.9 | 3.6 | 3.8 | 4.2 | 2.9 | — | — | — | — |
| alloy C | 60.2 | 16.6 | 7.5 | 6.0 | 7.0 | 2.7 | — | — | — | — |
| alloy D/ CM247LC $\gamma'$[26] | 69.4 | 15.5 | 5.8 | 3.4 | 2.3 | 2.1 | 1.4 | 0.1 | — | — |
| ME15 $\gamma'$[27] | 69.0 | 17.7 | 5.3 | 2.5 | 1.9 | 2.9 | — | 0.5 | 0.2 | — |
| RENE' N5 $\gamma'$[2] | 74.5 | 15.7 | 4.3 | 2.6 | 1.0 | 1.2 | — | 0.5 | 0.2 | — |
| RR2100 $\gamma'$[28] | 67.1 | 16.9 | 8.6 | 1.4 | 2.6 | 2.9 | — | — | 0.5 | — |
| RR2101 $\gamma'$[28] | 66.1 | 16.6 | 8.8 | 1.4 | 2.7 | 3.0 | — | — | 0.5 | 0.9 |

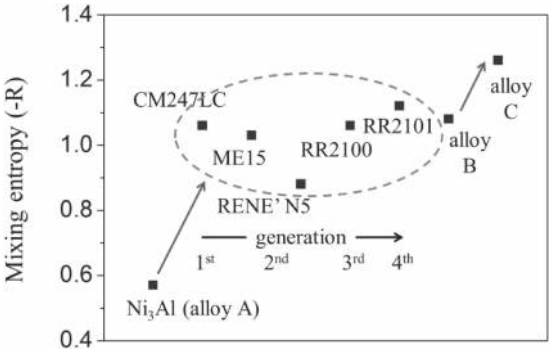


Fig. 3 The calculated mixing entropy ($\Delta S_{mix}$) of alloy A, B, C and some conventional Ni-based superalloys.

$$\Delta S_{mix} = -R(X_A \ln X_A + X_B \ln X_B + \cdots),$$

where $R$ is the gas constant, $X_A$ means the molar fraction of constituent A, $X_B$ means the molar fraction of constituent B, and so on. Review the development of Ni-based superalloys, the growing addition of Mo, W, Re and Ru all mainly partition to $\gamma$ matrix, so the mixing entropy of $\gamma'$ phase from 1st to latter generation superalloys still keeps at a lower level (Fig. 3). Therefore in present study, it is the first time to focus on evaluating the effect of increasing mixing entropy of $\gamma'$ phase.

### 3.2 Thermal stability of $\gamma'$ phase

Figure 4 shows the XRD results of the (100) and (110) ordered FCC peaks in alloy A to C after 1100, 1200 and 1300°C aging. According to JCPDS card, the intensity of (100) and (110) ordered FCC peaks were considerably lower than the main peaks such as (111) and (200). After such high temperature treatment, some weak intensity peaks may be interfered by the other strong intensity peaks. Therefore not all the (100) and (110) ordered peaks both presented at the same time in the XRD results. In addition, after different aging temperature the specimens were scanned at least two times at different positions for minimizing the effect of preferred-orientation.

The ordered FCC peaks of all three alloys exist after 1100 and 1200°C aging, but the peak has disappeared after 1300°C aging in alloy C. In addition, the intensity of ordered peaks in alloy B weakens significantly indicating that the order-disorder transition was in the process. The order-disorder transition temperature of $Ni_3Al$ alloy is slightly lower than its melting temperature which is about 1375°C.[29] The $\gamma'$ disordering temperature decreases from alloy A to C, and this proves that the higher randomness of atomic distribution in $\gamma'$ lattice can reduce its thermal stability. Similar result of decrement in order-disorder transition temperature was also reported. The disordering temperature of $Ni_3Al$ alloy decreases significantly with minor Fe addition.[30]

The DTA measurement results of alloy A to C from 1240 to 1400°C are shown in Fig. 5. The solidus temperature of

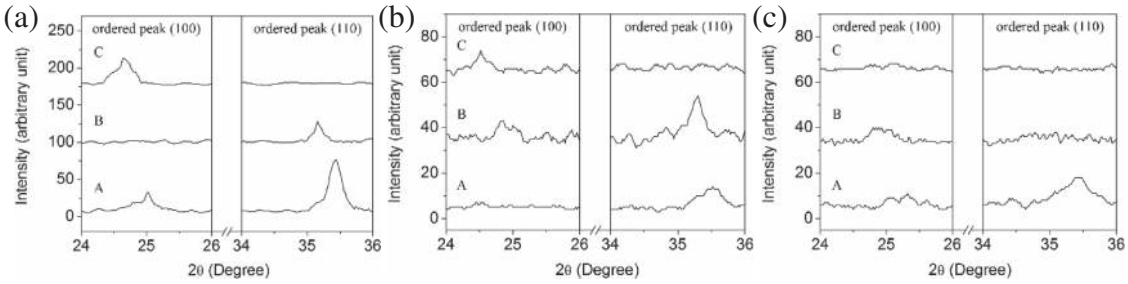


Fig. 4 The XRD results of alloy A, B and C after (a) 1100, (b) 1200 and (c) 1300°C heat treatment.

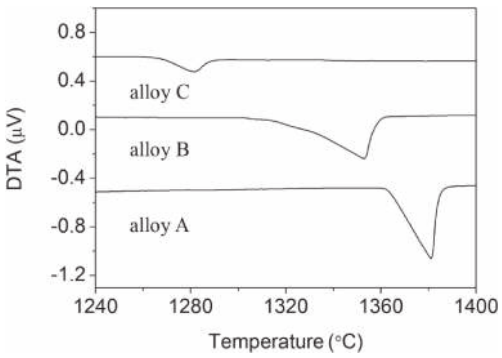


Fig. 5 The DTA results from 1240 to 1400°C of alloy A, B and C.

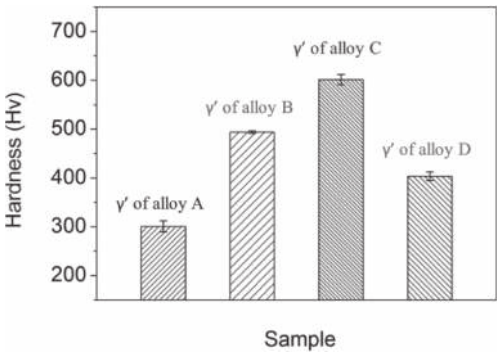


Fig. 6 The micro-hardness of $\gamma'$ in alloy A, B, C and D.

alloy A is about 1367°C, and for alloy B, the solidus temperature of $\gamma'$ is 1316°C. The $\gamma'$ solidus temperature in alloy C has been further reduced to about 1258°C. Although there are $\beta$, W-rich BCC, Laves phases present in alloy B and C, thermal aging experiments have confirmed that the solidus temperatures of $\gamma'$ phases in present study shows a trend of decrease with higher mixing entropy. It is interesting that the melting temperatures of Co, Cr, Ta and W (1495, 1907, 3017 and 3422°C, respectively) are all higher than that of $Ni_3Al$. From the rule of mixture, the $\gamma'$ solidus temperature should be increased. However, the higher alloying in $Ni_3Al$ also lowers its thermal stability.

### 3.3 Micro-hardness analysis of $\gamma'$ phase

In order to evaluate the strengthening effect from higher entropy system, micro-hardness analysis has been conducted on the $\gamma'$ phase region in alloy A, B and C. For comparisons, single phase $\gamma'$ of CM247LC has been prepared by the same mean and its hardness is also tested. The $\gamma'$ composition of CM247LC was reported in our previous work,[26] and it is listed in Table 2 (named alloy D here); SEM and XRD analysis have shown that alloy D contains mainly $\gamma'$ phase (Fig. 1(d) and 2(d)). The lattice constant of alloy D is estimated to be 0.3582 nm, which is close to the $a_{\gamma'}$ calculated from Vegard's Law (0.3589 nm). The micro-hardness of $\gamma'$ phase from alloy A to D are plotted in Fig. 6, and the results show that the hardness values are significantly increased with higher alloying (300.4, 494.0 and 601.4 Hv for sample A, B and C, respectively). The value of alloy D is about 401.9 Hv, which is lower than that of alloy B and C. It shows that the hardness of $\gamma'$ phase with higher $\Delta S_{mix}$ can surpass those in traditional superalloys due to higher degree of solid-solutions. This significant strengthening effect in $\gamma'$ indicates that designing Ni-based superalloys toward higher mixing entropy can be expected helpful for improving their mechanical performances.

### 3.4 Discussions

#### 3.4.1 $\gamma'$ composition and thermal stability

In present study, the $\Delta S_{mix}$ of $\gamma'$ phase has been elevated by alloying Co, Cr, Ta and W to the base composition $Ni_3Al$. With considerable quantities of alloying additions, the maximum randomness of atomic occupancy in $Ni_3Al$ $L1_2$ ordered lattice was proposed previously;[31] the content of Ni and Al should excess 25 and 6.25 at% in order to maintain the symmetry of atomic distribution for lowest degree of ordering. The content of Ni and Al in $\gamma'$ phase of present alloy B and C are far beneath these limits, hence the ordering can be retained as experimental results have shown.

In terms of thermal stability, according to DTA and XRD results, the thermal stability of $\gamma'$ can be decreased with higher $\Delta S_{mix}$. The reason might be due to the random atomic distribution interfering the bonding in ordered structure. Based on the binary mixing enthalpies of constituent elements listed in Table 3, when the main bonding such as Ni-Al and Ni-Ta in $Ni_3(Al, Ta)$ $\gamma'$ is substituted by Co-Al, Co-Ta and even others, the enthalpy will decrease and thus result in weaker bonding. JMATPRO software (Ni alloys database)[32] has been utilized for calculating the ordering enthalpy of $\gamma'$ phase from alloy A to C. The enthalpy of $\gamma'$ formation at 1000°C is calculated against the enthalpy of mixing of the FCC phase with the measured compositions. The calculated values are −6.4, −6.2 and −5.7 kJ/mole for alloy A, B and C, respectively. These calculations suggest that the $\gamma'$ ordering energy would influence its thermal stability, so it is important to retain high $\gamma'$ ordering enthalpy

Table 3 The mixing enthalpies (kJ/mol) of binary atomic pair.[33)]

| $\Delta H_{mix}$ | Ni | Al | Co | Cr | Ta | W |
|---|---|---|---|---|---|---|
| Ni | — | −22 | 0 | −7 | −29 | −3 |
| Al | −22 | — | −19 | −10 | −19 | −2 |
| Co | 0 | −19 | — | −4 | −24 | −1 |
| Cr | −7 | −10 | −4 | — | −7 | +1 |
| Ta | −29 | −19 | −24 | −7 | — | −7 |
| W | −3 | −2 | −1 | +1 | −7 | — |

when introducing high entropy strengthening for Ni-based superalloys in the future.

### 3.4.2 Strengthening of $\gamma'$ phase

In conventional Ni-based superalloys, alloying additions such as Mo, W, Re and Ru are responsible to improve the mechanical properties, however, these elements are mainly solutes in $\gamma$ phase. On the contrary, $\gamma'$ compositions have evolved not as significantly as those of $\gamma$ throughout the evolution of Ni-based superalloy compositions. According to Fig. 3, it is clear that the $\Delta S_{mix}$ of $\gamma'$ phase in Ni-base superalloys has not changed much. Therefore the strengthening of $\gamma'$ phase is also a critical issue that needs to be addressed. Through higher alloying in $\gamma'$, the hardness can be markedly enhanced. Compare the hardness of alloy C and alloy D (601.4 and 401.9 Hv), the $\gamma'$ strength is 1.5 fold higher for alloy C. Higher degree of lattice distortion can be one of the underlying mechanisms for strengthening. The extent of lattice distortion in multi-element alloy system can be calculated from following formula:[34)]

$$\delta = 100\sqrt{\sum_{i=1}^{n} c_i\left(1-\frac{r_i}{\bar{r}}\right)^2},$$

where $\bar{r} = \sum_{i=1}^{n} c_i r_i$ and $c_i$, $r_i$ are the atomic percentage, atomic radius of $i_{th}$ element. The $\delta$ value calculated from the $\gamma'$ composition in alloy C is 6.01, while that of CM247LC (alloy D) is 5.68. Hence the stronger lattice distortion may contribute to higher $\gamma'$ hardness. Furthermore, the strengthening of $\gamma'$ phase is also related to the magnitude of anti-phase boundary (APB) energy.[3)] The APB energy variation of ternary addition Ta in $Ni_3Al$ alloy has been proposed by first-principle calculation,[35)] and the Ta substitutes with Al can markedly change the APB energy of $\gamma'$ phase. The APB energy of $Ni_3Al$ alloy is about 181 $mJ/m^2$ of (111) plane. For $Ni_3Al_{1-x}Ta_x$ system, the APB energy stays nearly constant with $x \leq 0.2$, and abruptly increases when $x > 0.2$. It reaches to the maximum APB energy (about 600 $mJ/m^2$) when $x$ is in the range of 0.25 to 0.5. After $x > 0.5$, the APB energy gradually falls and indicates that the formation of APB becomes more unstable. According to the $Ni_3Al_{1-x}Ta_x$ of $\gamma'$ in alloy C, the $x$ is about 0.3 so the APB energy of $\gamma'$ in alloy C may reach to about 600 $mJ/m^2$. In contrast, the Ta content of $\gamma'$ phase in conventional Ni-based superalloys is much lower, so less enhancement in APB energy. From JMATPRO calculation, the APB energy of $\gamma'$ in CM247LC is only around 200 $mJ/m^2$, that is much lower than that of $\gamma'$ in alloy C. Therefore, the highly alloyed $\gamma'$ phase can possess higher resistance against plastic deformation due to enhanced lattice distortion and higher APB energy.

Increasing the mixing entropy of alloys implies strong solid-solution strengthening. So, solid-solution strengthening of Ta and the strengthening due to higher mixing entropy are related. Furthermore, the increase of anti-phase boundary (APB) energies due to Ta addition can contributes to the significant increase in hardness. According to the $Ni_3Al_{1-x}$-$Ta_x$ of alloy B, the $x$ is only 0.17, so the enhancement of APB energy from alloy A to B would not be so obvious. Consequently, the additional $\gamma'$ hardness (about 200 Hv) from alloy A to B mainly can result from the strengthening by elevated mixing entropy (lattice distortion). As for the $\gamma'$ hardness increment from alloy B to C, the additional 100 Hv can be attributed to both further solid-solution strengthening and the increase in APB energy. So, choosing the right element to increase the entropy term is critical for improving the strength of $Ni_3Al$ $\gamma'$.

## 4. Conclusion

The mixing entropy of ordered $\gamma'$ has been elevated to study its effects on thermal stability and hardness. Improvement in hardness can be achieved due to lattice distortion strengthening and higher anti-phase boundary energy of $\gamma'$. On the other hand, the thermal stability of gamma prime phase is decreased due to greater disordering.

## Acknowledgements

Authors would like to thank the financial support from Ministry of Science and Technology, Taiwan (R.O.C.), project grant number: 103-2221-E-214-035, 103-2218-E-007-019. Special thanks to Prof. J.W. Yeh for discussions about high entropy alloys.

## REFERENCES

1) P. Caron and T. Khan: Aerosp. Sci. Technol. **3** (1999) 513–523.
2) T. M. Pollock and S. Tin: J. Propul. Power **22** (2006) 361–374.
3) R. C. Reed: *The Superalloys: Fundamentals and Applications*, (Cambridge University Press, 2006).
4) C. J. Mcmahon and L. F. Coffin: Metall. Trans. **1** (1970) 3443–3450.
5) A. Staroselsky and B. N. Cassenti: Int. J. Solids Struct. **48** (2011) 2060–2075.
6) A. K. Sinha: Prog. Mater. Sci. **15** (1972) 81–185.
7) R. C. Reed, M. P. Jackson and Y. S. Na: Metall. Mater. Trans. A **30** (1999) 521–533.
8) J. X. Zhang, T. Murakumo, Y. Koizumi, T. Kobayashi, H. Harada and S. Masaki: Metall. Mater. Trans. A **33** (2002) 3741–3746.
9) A. C. Yeh and S. Tin: Scr. Mater. **52** (2005) 519–524.
10) A. Yeh and S. Tin: Metall. Mater. Trans. A **37** (2006) 2621–2631.
11) K. Kawagishi, A. Sato, H. Harada, A. C. Yeh, Y. Koizumi and T. Kobayashi: Mater. Sci. Technol. **25** (2009) 271–275.
12) J. W. Yeh, S. K. Chen, S. J. Lin, J. Y. Gan, T. S. Chin, T. T. Shun, C. H. Tsau and S. Y. Chang: Adv. Eng. Mater. **6** (2004) 299–303.
13) J. W. Yeh, S. K. Chen, J. Y. Gan, S. J. Lin, T. S. Chin, T. T. Shun, C. H. Tsau and S. Y. Chang: Metall. Mater. Trans. A **35** (2004) 2533–2536.
14) B. Cantor, I. T. H. Chang, P. Knight and A. J. B. Vincent: Mater. Sci. Eng. A **375** (2004) 213–218.
15) W. H. Wu, C. C. Yang and J. W. Yeh: Annal. Chimi. Sci. Mater. **31** (2006) 737–747.
16) J. W. Yeh: Annal. Chimi. Sci. Mater. **31** (2006) 633–648.
17) M. H. Chuang, M. H. Tsai, W. R. Wang, S. J. Lin and J. W. Yeh: Acta Mater. **59** (2011) 6308–6317.
18) K. Y. Tsai, M. H. Tsai and J. W. Yeh: Acta Mater. **61** (2013) 4887–

4897.
19) S. Ochiai, Y. Oya and T. Suzuki: Acta Metall. **32** (1984) 10.
20) Y. Mishima, S. Ochiai and T. Suzuki: Acta Metall. **33** (1985) 1161–1169.
21) A. J. Bradley and A. Taylor: Proc. R. Soc. Lond. A—Math. Phys. Sci. **159** (1937) 56–72.
22) A. Taylor and R. W. Floyd: J. Inst. Metals **80** (1952) 577.
23) R. W. Guard and J. H. Westbrook: Trans. Am. Inst. Min. Metall. Eng. **215** (1959) 807–814.
24) K. Aoki and O. Izumi: Phys. Status Solidi (a) **38** (1976) 587–594.
25) P. V. M. Rao, K. S. Murthy, S. V. Suryanarayana and S. V. N. Naidu: Phys. Status Solidi (a) **133** (1992) 231–235.
26) A. C. Yeh, K. C. Yang, J. W. Yeh and C. M. Kuo: J. Alloy. Compd. **585** (2014) 614–621.
27) Y. Amouyal and D. N. Seidman: Acta Mater. **59** (2011) 6729–6742.
28) R. C. Reed, A. C. Yeh, S. Tin, S. S. Babu and M. K. Miller: Scr. Mater. **51** (2004) 327–331.
29) R. W. Cahn, P. A. Siemers, J. E. Geiger and P. Bardhan: Acta Metall. **35** (1987) 2737–2751.
30) F. J. Bremer, M. Beyss and H. Wenzl: Phys. Status Solidi (a) **110** (1988) 77–82.
31) T. T. Shun, C. H. Hung and C. F. Lee: J. Alloy. Compd. **493** (2010) 105–109.
32) N. Saunders, Z. Guo, X. Li, A. P. Miodownik and J. P. Schille: JOM **55** (2003) 60–65.
33) A. Takeuchi and A. Inoue: Mater. Trans. **46** (2005) 2817–2829.
34) S. Guo, Q. Hu, C. Ng and C. T. Liu: Intermetallics **41** (2013) 96–103.
35) M. Chandran and S. Sondhi: Model. Simul. Mater. Sci. Eng. **19** (2011) 025008.